Spinal cerebrospinal fluid flow is increased in rats with elevated intracranial pressure 18 hours after cortical ischaemic stroke

Steven William Bothwell
University of Newcastle https://orcid.org/0000-0002-0861-1661
Daniel Omileke
University of Newcastle
Debbie-Gai Pepperall
University of Newcastle
Adjanie Patabendige
University of Newcastle
Neil J Spratt (Neil.Spratt@health.nsw.gov.au)
The University of Newcastle, Hunter Medical Research Institute, Hunter New England Local Health District https://orcid.org/0000-0002-9023-6177

Research

Keywords: Cerebrospinal fluid, infarct expansion, ischaemia, intracranial pressure, stroke

Posted Date: October 1st, 2020

DOI: https://doi.org/10.21203/rs.3.rs-84123/v1

Abstract

Background A dramatic oedema-independent intracranial pressure (ICP) rise occurs 24 hours post-stroke in rats and may explain infarct expansion. Underlying mechanisms of this rise are unknown but evidence suggests cerebrospinal fluid (CSF) dynamics are involved. Methods We investigated how CSF flow changes post-stroke and how this relates to ICP by infusing CSF tracer into the lateral ventricles of rats and assessing transport time and total tracer transport to the spinal subarachnoid space over a 90 minute period. Results Stroke animals with ICP rise had faster tracer transit when compared with stroke animals without ICP rise (27.6 ± 4, n = 6, vs 48.6 ± 4.5 mins, n = 6) or animals subjected to a sham procedure (47.9 ± 4 mins, n = 8), $F(2,17) = 0.1$, $p \leq 0.01$. There was a correlation between tracer transit time and ΔICP ($R = -0.52$, $p=0.02$) and infarct volume ($R = -0.6$, $p=0.04$). There was no difference in total tracer observed. Conclusions Faster tracer transit in stroke animals may be explained by impairment of other CSF outflow pathways, whereby, spinal drainage acts as a compensatory mechanism. Investigation into the disruption of other CSF drainage routes post-stroke may offer insight into the underlying mechanisms of infarct expansion post-stroke.

Background

Ischaemic stroke is a leading cause of death and disability worldwide [1]. Stroke severity is variable and some patients present with relatively minor stroke. While occlusion of small branch vessels accounts for many of those with minor symptoms, it is now recognised that some patients with minor symptoms may have large vessel occlusion [2]. Around 10–20% of patients with minor stroke or transient ischaemic attack will experience early recurrent stroke, and the vast majority of these occur in the initially ischaemic vascular territory [3, 4].

The most likely cause of infarct expansion is failure of leptomeningeal collateral vessels. Failure of initially good collateral blood flow is associated with infarct growth following ischaemic stroke [5]. The cause of collateral vessel failure has not been definitively established. However, after stroke, blood flow in these vessels is largely driven by cerebral perfusion pressure (CPP) which is sensitive to changes in intracranial pressure (ICP) [6]. In support of this, our previous work showed that elevation of ICP during middle cerebral artery occlusion (MCAo) in rats caused a linear reduction of collateral blood flow [7]. We previously identified a transient but dramatic rise in ICP 24 hours after minor ischemic stroke in rats [8]. For the first time, this study reported ICP rise after minor ischemic stroke. The time point of this ICP rise, taken with our understanding of how ICP influences collateral blood flow, suggests a possible mechanism of collateral failure and infarct expansion.

Our understanding of the underlying mechanisms of this ICP rise is limited. We know that oedema is not the primary cause [9] and pilot data from our lab found no contribution of cerebral blood volume [unpublished data]. Resistance to CSF outflow is increased at 18 hours post-stroke in a rat model of cortical ischaemia and at 24 hours post-stroke in a model of striatal ischaemia [10, 11]. This suggests that CSF volume is increased at these time points.

The relative importance and contribution of CSF drainage pathways are not well defined [12]. CSF drains from the cerebral ventricular system to the spinal subarachnoid space and canal before moving into lymphatic vessels of the sacral spine [13, 14]. This offers an opportunity to image CSF dynamics *in vivo* by focusing on spinal CSF flow. In this study, we evaluated how spinal CSF flow is altered post-stroke and whether this is related to ICP rise. We aimed to determine whether CSF flow from the cranium to the spinal subarachnoid space is impaired after stroke and whether this relates to ICP rise.

Methods

Animals

Procedures were carried out on male outbred Wistar rats aged between 8 and 12 weeks (n = 20) weighing between 280–320 g. All experimental animal procedures used in this project were in accordance with the Australian Code of Practice for the Care and Use of Animals for Scientific Purposes and were approved by the Animal Care and Ethics Committee of the University of Newcastle (A-2013-343). The studies were conducted and the manuscript prepared in accordance with the ARRIVE guidelines [15].

Animals were excluded from experiments if they presented with congenital deformities that obstructed surgical intervention. Animals were only involved in the analysis following confirmation of stroke and ventricle penetration of infusion catheter after histology.

Animals were assigned to stroke or sham groups on day 0, prior to intervention. Blinding was not carried out during experimental procedures; however, the investigator was blinded at the time of data extraction and analysis: each animal was assigned an experiment number and analysis was carried out on all data in one sitting with no indication of treatment to the investigator. Five animals per group were required to detect a 30% change in CSF tracer transit between stroke and sham animals with 80% power and α error probability of 0.05 (SD = 6.2). Power calculations were conducted on pilot data using power calculation software (G*Power 3.1.9.2). Pilot data was included in the final analysis.

Anaesthesia and monitoring

Rats were anaesthetised with isoflurane (5% induction, 2-2.5% maintenance) in 50:50% N_2:O_2. Incision sites were injected subcutaneously (s.c.) with 2 mg/kg 0.05% Bupivacaine (Pfizer, Sydney, Australia). Core body temperature was regulated via a thermocouple rectal probe (RET-2, Physitemp Instruments Inc, Clifton, New Jersey, USA) and heat mat. Blood gases were monitored on day 0 prior to stroke and day 1 prior to laminectomy from 0.1 ml blood samples from a femoral arterial line. This line was also used for arterial blood pressure monitoring. Prior to recovery, an additional Bupivacaine injection (0.3 ml, 0.05%, s.c.) and rectal paracetamol (250 mg/kg; GlaxoSmithKline, Brentford, UK) were administered for overnight pain relief. Saline was administered intraperitoneally (2 × 1.5 mL) to replace fluid loses. Following surgery, animals were returned to their cages with free access to food and water. Cages were placed half over a heat mat to allow animals to thermoregulate during recovery.

ICP measurement

ICP was measured using a fibre-optic pressure sensor (Opsens Solutions, Quebec, Canada). The wire was sealed 5 mm inside a hollow saline-filled screw in the left parietal bone (-1.8 mm lateral and − 2 mm posterior to Bregma). Correct positioning was confirmed when a trace of pulse and respiratory oscillations were observed after the wire was sealed in place. Baseline ICP was recorded for 30 minutes prior to photothrombotic stroke, and day 1 ICP was recorded from 18 to 21 hours.

Photothrombotic stroke

A light source (100,000 LUX, 5 mm diameter, Olympus Corporation LG-PS2, Tokyo, Japan) was placed over the right parietal bone 0.5 mm from the skull surface, 1.2 mm posterior to Bregma. While the light source was concentrated on the skull, Rose Bengal in saline (0.01 g/kg; Sigma, St Louis, Missouri, USA) was infused into the right femoral vein followed by 1 mL saline. The light source remained constant for 20 minutes after Rose Bengal infusion. Sham animals were administered saline alone.

Laminectomy

Laminectomy was carried out as previously described [16]. Briefly, an incision was made from the back of the head caudally to the mid-thoracic region. The connective tissue was blunt dissected away and a cut was made through the midline of each muscle layer. The paraspinous muscles were retracted to expose the spinal column and connective tissue was blunt dissected. A dental drill (Saeshin Precision, Paho-dong, Korea) was used to thin the laminae of the C7 and T1 vertebrae. The laminae were then cut and removed at these points to expose the spinal cord.

Evans blue infusion

Evans blue was infused bilaterally into the lateral ventricles (2% w/v in aCSF, 20 µL total volume, 2 µL/min). Intraventricular catheters were sealed in head screws positioned 0.8 mm posterior and 1.8 mm lateral to Bregma on both parietal bones. The catheters were connected to two syringes containing Evans blue and infusion was controlled by a syringe driver (Harvard Apparatus, Holliston, MA, USA). Penetration of the ventricles was later confirmed by histology.

Image acquisition and ImageJ analysis

Images were acquired using a standard microscopic eyepiece camera connected to a PC running basic image acquisition software. An image was captured every minute for 90 minutes. These images were then loaded into ImageJ as a sequence. The images were converted to an 8-bit format with the colour channels split; only the red channel was used for analysis as this minimised contrast from blood vessels. Two regions of interest were selected: the spinal cord and an area out-with the spinal cord to correct for background noise. Difference between each image and baseline were calculated to show contrast development.

Histological Analysis

The animal was euthanised at 3 hours post-infusion and was transcardially perfused with 0.9% saline. The brains were then fixed in neutral-buffered formalin before being processed and paraffin embedded.

Coronal sections of 5 and 10 μm were cut and stained with hematoxylin and eosin. Images were scanned using a digital slide scanner (Aperio Technologies, Vista, CA, USA) and image analysis was carried out within the Aperio programme. Image analysis was confirmed by an independent investigator and any cases with > 10% discrepancy were flagged for review.

Experimental design

The experimental timeline is outlined in Fig. 1. Physiological variables were recorded at baseline on day 0 prior to photothrombotic stroke and at 18 hours post stroke, prior to surgical intervention. Screws were placed over the lateral ventricles and a dental cap fitted on day 0, ready for infusion the following day. A C7-T1 laminectomy was performed on day 1 to expose this area of the spinal cord. Bilateral infusion of Evans blue into the lateral ventricles took place at 18 hours post-stroke. White light images were acquired of the C7-T1 spinal cord every 60 seconds from zero to 90 minutes post-infusion and images were analysed using ImageJ software (NIH). The animals were sacrificed at 3 hours post-infusion and histological analysis was carried out as described.

Although we previously reported a transient ICP rise at 24 hours post-stroke [9], we chose 18 hours post-stroke as our time point for this investigation. This is because we would expect any changes to CSF flow to be present at this earlier time point, which would contribute to the ICP rise we observe later. If we investigate CSF changes at 22 to 24 hours, there is a high likelihood of missing these changes, as we would expect the system to start to return to baseline levels at this point.

[Insert Fig. 1]

Statistical analysis

Statistical analyses were carried out using GraphPad Prism 7 (GraphPad Software, La Jolla, CA, USA). Data was tested for normal distribution using a D'Agostino and Pearson normality test. Comparisons between two groups were analysed by unpaired Student's t-test for normally distributed data and by Mann-Whitney U-test for non-normally distributed data. Comparisons between three or more groups were carried out using one-way ANOVA. All normally distributed data values are presented graphically as average ± standard deviation and non-normally distributed data as median and interquartile range (IQR). Relationships were determined by Pearson correlation unless otherwise stated.

Results

Table 1 shows the physiological parameters of stroke and sham animals on day 0 and day 1.

Table 1
Physiological Parameters

	Stroke with ICP rise		Stroke no ICP rise		Sham	
	Day 0 (Baseline)	**Day 1**	**Day 0**	**Day 1**	**Day 0**	**Day 1**
Respiratory rate (BPM)	61.7 ± 3.2	59.7 ± 3.2	66.7 ± 6.4	68.5 ± 5.6	63.5 ± 2.8	69.8 ± 6.7
Heart rate (BPM)	442 ± 14	428 ± 28	444 ± 23	418 ± 37	425 ± 12	418 ± 20
Mean arterial pressure (mmHg)	92.1 ± 4.7	91.9 ± 3.8	91.4 ± 8.9	95.6 ± 9.1	87.8 ± 7.7	87.0 ± 7.1
SpO_2 (%)	97.9 ± 1.0	98.0 ± 2.4	97.0 ± 2.7	97.9 ± 2.4	98.9 ± 1.1	97.8 ± 2.8
paO_2 (mmHg)	184 ± 25	204 ± 27	169 ± 28	192 ± 36	150 ± 23	194 ± 23
$paCO_2$ (mmHg)	61.5 ± 9.1	64 ± 9.8	53.8 ± 8.7	59.2 ± 6.1	63.6 ± 5.9	61.8 ± 7.9
pH	7.28 ± 0.04	7.31 ± 0.04	7.30 ± 0.04	7.32 ± 0.02	7.25 ± 0.01	7.30 ± 0.04

Exclusions

Three animals were excluded from experimentation as they presented with congenital deformities that prevented surgical intervention. Four animals were excluded due to technical errors during procedures and one animal died before the procedure could be completed.

ICP rise occurred in six out of 12 stroke animals

ICP rise (≥ 5 mmHg) occurred in stroke animals but not sham (Fig. 2). ΔICP was significantly higher in stroke animals (3.53 mmHg, IQR = 0.06 to 9.41) than in sham animals (-0.71 mmHg, IQR = -2.47 to 1.09 n = 8), U = 19, p = 0.025. We found that 6/12 stroke animals had an ICP rise between baseline (day 0) and 18 hours post-stroke, and there was a clear bimodal distribution from those that did not have a rise. For subsequent analyses to determine whether there was an association between ICP rise and CSF flow, we separated stroke animals into two groups depending on whether they had an ICP rise or not.

[Insert Fig. 2]

Stroke animals with ICP rise had increased CSF flow compared to stroke animals with no ICP rise or sham animals

CSF flow rate, represented by time to reach 50% maximum contrast (T50%max), was similar between stroke animals with no ICP rise (48.6 ± 4.5 min, n = 6) and sham animals (47.9 ± 4 min, n = 8). T50%max

was significantly lower for stroke animals with ICP rise (27.6 ± 4 min, n = 6) compared to the other groups (Fig. 3A), $F(2, 17) = 0.1$, $p \leq 0.01$.

We found a significant inverse correlation between ΔICP and T50%max. Animals with a higher ΔICP reached 50% maximum contrast faster than those with a lower ΔICP, $R = -0.52$, $p = 0.02$, Spearman's correlation (Fig. 3B).

[Insert Fig. 3]

Increased infarct volume correlates with increased CSF flow

We found that there was a strong trend to a correlation between infarct volume and ΔICP from baseline to 18 hours post-stroke, although not statistically significant (Fig. 4A), $R = 0.55$, $p = 0.07$, Spearman's correlation. However, we identified a significant correlation between infarct volume and T50%max, which demonstrates faster transit of Evans blue to the C7-T1 spinal subarachnoid space in animals with larger infarct volumes (Fig. 4B), $R = -0.6$, $p = 0.04$.

[Insert Fig. 4]

Maximum contrast did not differ between groups

To estimate the contribution of CSF secretion to changes in CSF flow, we determined the maximum change in contrast from 0 to 90 minutes post-infusion for each animal (Fig. 5A). The maximum change in contrast did not significantly differ between stroke animals with ICP rise (175.2 ± 15.4 Arbitrary Units (AU), n = 6), stroke animals without ICP rise (152 ± 18.1 AU, n = 6), and sham animals (125.1 ± 16.7 AU, n = 8), $F(2, 17) = 2.28$, $p = 0.13$.

[Insert Fig. 5]

Oedema is not the cause of ICP rise 18-hours after photothrombotic stroke

We asked whether oedema could explain the elevated ICP at 18 hours post-stroke. Oedema did not correlate with ΔICP between baseline and 18 hours post-stroke (Fig. 6A), $R = 0.41$, $p = 0.18$, Spearman's correlation. Further, oedema volume did not correlate with T50%max (Fig. 6B), $R = -0.12$, $p = 0.7$.

[Insert Fig. 6]

Discussion

In this study, we demonstrated that CSF flow from the cranial compartment to the spinal subarachnoid space is faster after stroke. We observed that oedema-independent ICP rise is present 18 hours after cortical photothrombotic stroke in rats and that this ICP rise correlates to faster movement of CSF tracer to the spinal subarachnoid space.

Resistance to CSF outflow is increased at 18 and 24 hours post-stroke in cortical and striatal ischaemia models, respectively [10, 11]. We expected stroke animals to have decreased and delayed movement of CSF tracer to the spinal subarachnoid space, indicative of impaired and slowed CSF movement which would possibly explain ICP rise at 24 hours post-stroke [9]. Our data show that animals experiencing an ICP rise post-stroke had faster transit of CSF tracer to the spinal subarachnoid space, while animals that did not experience ICP rise post-stroke were similar to sham animals. This observation was further confirmed when we identified a correlation between ICP rise at 18 hours post-stroke and Evans blue transit time to the C7-T1 spinal subarachnoid space. These findings show that changes to CSF flow post-stroke are linked to ICP rise; however, it remains unclear if ICP rise is the direct result of these changes or vice versa. Previous studies have observed increased transport of CSF tracer into the extracranial lymphatics system and through arachnoid projections with increased ICP [17, 18]. It is possible that increased CSF transit to the spinal subarachnoid space occurs in response to ICP rise following impaired CSF drainage via another cranial drainage pathway post-stroke. This is a possible compensatory mechanism given that CSF drains along spinal nerve routes extending from intervertebral spaces and into the peripheral lymphatics located in the sacral spine [14].

Despite faster transit to the C7-T1 subarachnoid space, the maximum amount of tracer present at this region between 0 to 90 minutes post-infusion was not significantly different. The lack of significant difference between the groups suggests that increased CSF secretion may not be involved in the ICP rise we observe. If CSF secretion was increased in animals experiencing ICP rise, then we would expect maximum observed contrast to be lower as the tracer becomes more dilute.

We investigated whether oedema could be the underlying cause of ICP elevation at 18 hours post-stroke, perhaps contributing to faster Evans blue transport to the spinal subarachnoid space. We found that oedema volume did not correlate with either ΔICP rise or T50%max. This finding is in line with our previous report that oedema does not correlate with ICP rise at 24 hours after transient MCAo [9] and with work showing similar observations after permanent MCAo [11]. Oedema volumes were assessed early and would likely be greater at later time points. However, we still observe ICP rise from 18 to 21 hours, which suggests that mechanisms other than oedema contribute to ICP rise and increased tracer movement after photothrombotic stroke.

In this study, 6 out of 12 stroke animals had ICP rise 18 hours post-stroke. This ICP rise was smaller than we previously reported with MCAo at 24 hours and photothrombotic stroke at 22 to 24 hours post-stroke [8, 9, 19]. Here, we used a photothrombotic technique to produce a cortical ischaemia instead of a striatal ischaemia. This was the preferred model for our study of CSF flow as we aimed to maintain choroid plexus integrity throughout our experiments. MCAo, a striatal stroke model, reduces blood flow to the

choroid plexus by around 62% and causes choroidal oedema leading to reduced blood-CSF barrier integrity and increased CSF secretion [20]. Further, the earlier time point of our investigation may explain the smaller ICP rise, as we would expect ICP to continue to rise and peak at 22 hours post-stroke as previously observed [19]. We chose this time point to observe any changes that may contribute to ICP rise as we expect changes to reduce later as the system returns to normal.

Experiments to elucidate physiological CSF dynamics are challenging and often involve some sort of intervention. In this study, we infused the CSF tracer, Evans blue, directly into the lateral ventricles of the animals [18, 21, 22]. This type of intervention has the potential to disturb normal CSF dynamics; however, this technique is widely used and we took care to limit the infusion rate to lower than that of CSF production (2.66–2.84 µl/min) to maintain the integrity of the system as much as possible [23].

Several CSF drainage hypotheses have been presented in recent years and we are yet to meet a consensus on the topic [24–26]. In recent years, lymphatic drainage of CSF from both the cranium and the spinal space have gained merit in the field, with several groups demonstrating the presence of CSF tracers in the peripheral lymphatic system, primarily the cervical lymphatics [21, 27–30]. This may be an interesting direction of investigation to understand how CSF drainage is altered post-stroke.

Conclusions

Overall, we demonstrate that CSF flow from the cranial compartment to the spinal subarachnoid space is increased 18 hours post-stroke. Taken with our observation of increased resistance to CSF outflow at 18 hours post-stroke [10] and that oedema does not correlate to ICP rise or Evans blue transit, we believe that altered CSF movement and drainage from the CNS contributes to ICP rise post-stroke. This hypothesis must be further explored to elucidate the exact changes to CSF dynamics that occur. These changes may offer insight into the underlying mechanism of ICP elevation and collateral failure and could be used as a therapeutic target to improve patient outcome after minor ischaemic stroke.

Abbreviations

- ICP – Intracranial pressure
- CSF – Cerebrospinal fluid
- MCAo – Middle cerebral artery occlusion

Declarations

Acknowledgements

Not applicable.

Funding

This study was supported by an HDR scholarship to SB by the University of Newcastle, Australia. AP is supported by the NSW Ministry of Health under the NSW Health Early-Mid Career Fellowships Scheme. NJS was supported by a co-funded Australian NHMRC/NHF Career Development/Future Leader Fellowship [GNT1110629/ 100827]

Ethics approval

All experimental animal procedures used in this project were in accordance with the Australian Code of Practice for the Care and Use of Animals for Scientific Purposes and were approved by the Animal Care and Ethics Committee of the University of Newcastle (A-2013-343).

Authors' contributions

SB carried out the surgical components of the study, analysed and interpreted the data, performed statistical analysis and drafted the manuscript. DO and DP helped with histology and image analysis. NJS and AP participated in the concept and design of the study, helped with interpretation of the data and drafting the manuscript, and contributed equally. All authors read and approved the final manuscript.

Availability of data and materials

The data generated during this study are available from the corresponding author on reasonable request.

Consent for publication

Not applicable.

Competing interests

The authors declare that they have no competing interests.

References

1. WHO. Projections of mortality and burden of disease. 2002–2030.
2. Smith EE, Abdullah AR, Petkovska I, Rosenthal E, Koroshetz WJ, Schwamm LH. Poor outcomes in patients who do not receive intravenous tissue plasminogen activator because of mild or improving ischemic stroke. Stroke. 2005;36(11):2497–9.
3. Coutts SB, Modi J, Patel SK, Aram H, Demchuk AM, Goyal M, et al. What causes disability after transient ischemic attack and minor stroke?: Results from the CT and MRI in the Triage of TIA and minor Cerebrovascular Events to Identify High Risk Patients (CATCH) Study. Stroke. 2012;43(11):3018–22.
4. Asdaghi N, Hameed B, Saini M, Jeerakathil T, Emery D, Butcher K. Acute perfusion and diffusion abnormalities predict early new MRI lesions 1 week after minor stroke and transient ischemic attack. Stroke. 2011;42(8):2191–5.

5. Campbell BC, Christensen S, Tress BM, Churilov L, Desmond PM, Parsons MW, et al. Failure of collateral blood flow is associated with infarct growth in ischemic stroke. J Cereb Blood Flow Metab. 2013;33(8):1168–72.
6. Czosnyka M, Pickard JD. Monitoring and interpretation of intracranial pressure. J Neurol Neurosurg Psychiatry. 2004;75(6):813–21.
7. Beard DJ, McLeod DD, Logan CL, Murtha LA, Imtiaz MS, van Helden DF, et al. Intracranial pressure elevation reduces flow through collateral vessels and the penetrating arterioles they supply. A possible explanation for 'collateral failure' and infarct expansion after ischemic stroke. J Cereb Blood Flow Metab. 2015;35(5):861–72.
8. Murtha LA, McLeod DD, McCann SK, Pepperall D, Chung S, Levi CR, et al. Short-duration hypothermia after ischemic stroke prevents delayed intracranial pressure rise. Int J Stroke. 2014;9(5):553–9.
9. Murtha LA, McLeod DD, Pepperall D, Mccann SK, Beard DJ, Tomkins AJ, et al. Intracranial pressure elevation after ischemic stroke in rats: cerebral edema is not the only cause, and short-duration mild hypothermia is a highly effective preventive therapy. J Cereb Blood Flow Metab. 2015;35(4):592–600.
10. Patabendige A, MacKovski N, Pepperall D, Hood R, Spratt N. Correction to: A26 Cerebrospinal fluid outflow resistance is increased following small-moderate ischaemic stroke. Fluids Barriers of the CNS. 2019;16(1):22.
11. Alshuhri MS, Gallagher L, McCabe C, Holmes WM. Change in CSF Dynamics Responsible for ICP Elevation After Ischemic Stroke in Rats: a New Mechanism for Unexplained END? Transl Stroke Res. 2019.
12. Bothwell SW, Janigro D, Patabendige A. Cerebrospinal fluid dynamics and intracranial pressure elevation in neurological diseases. Fluids Barriers CNS. 2019;16(1):9.
13. Murtha LA, Yang Q, Parsons MW, Levi CR, Beard DJ, Spratt NJ, et al. Cerebrospinal fluid is drained primarily via the spinal canal and olfactory route in young and aged spontaneously hypertensive rats. Fluids Barriers CNS. 2014;11.
14. Ma Q, Decker Y, Muller A, Ineichen BV, Proulx ST. Clearance of cerebrospinal fluid from the sacral spine through lymphatic vessels. J Exp Med. 2019.
15. Kilkenny C, Browne W, Cuthill IC, Emerson M, Altman DG. Animal Research: Reporting in vivo Experiments—The ARRIVE Guidelines. Journal of Cerebral Blood Flow Metabolism. 2011;31(4):991–3.
16. Walker MJ, Walker CL, Zhang YP, Shields LB, Shields CB, Xu XM. A novel vertebral stabilization method for producing contusive spinal cord injury. J Vis Exp. 2015(95):e50149.
17. McComb JG, Davson H, Hyman S, Weiss MH. Cerebrospinal fluid drainage as influenced by ventricular pressure in the rabbit. Journal of neurosurgery. 1982;56(6):790–7.
18. Boulton M, Flessner M, Armstrong D, Mohamed R, Hay J, Johnston AM. Contribution of extracranial lymphatics and arachnoid villi to the clearance of a CSF tracer in the rat. Am J Physiol. 1999;276(3 Pt 2):R818-23.

19. Beard DJ, Logan CL, McLeod DD, Hood RJ, Pepperall D, Murtha LA, et al. Ischemic penumbra as a trigger for intracranial pressure rise - A potential cause for collateral failure and infarct progression? J Cereb Blood Flow Metab. 2016;36(5):917–27.
20. Ennis SR, Keep RF. The Effects of Cerebral Ischemia on the Rat Choroid Plexus. J Cereb Blood Flow Metab. 2006;26(5):675–83.
21. Maloveska M, Danko J, Petrovova E, Kresakova L, Vdoviakova K, Michalicova A, et al. Dynamics of Evans blue clearance from cerebrospinal fluid into meningeal lymphatic vessels and deep cervical lymph nodes. Neurol Res. 2018;40(5):372–80.
22. Norwood JN, Zhang Q, Card D, Craine A, Ryan TM, Drew PJ. Anatomical basis and physiological role of cerebrospinal fluid transport through the murine cribriform plate. Elife. 2019;8.
23. Chiu C, Miller MC, Caralopoulos IN, Worden MS, Brinter T, Gordon ZN, et al. Temporal course of cerebrospinal fluid dynamics and amyloid accumulation in the aging rat brain from three to thirty months. Fluids Barriers CNS. 2012;9(1):3.
24. Orešković D, Klarica M. The formation of cerebrospinal fluid: Nearly a hundred years of interpretations and misinterpretations. Brain Res Rev. 2010;64(2):241–62.
25. Orešković D, Radoš M, Klarica M. The recent state of a hundred years old classic hypothesis of the cerebrospinal fluid physiology. Croat Med J. 2017;58(6):381–3.
26. Semyachkina-Glushkovskaya O, Postnov D, Kurths J. Blood-Brain, Barrier. Lymphatic Clearance, and Recovery: Ariadne's Thread in Labyrinths of Hypotheses. Int J Mol Sci. 2018;19(12).
27. Ma Q, Ineichen BV, Detmar M, Proulx ST. Outflow of cerebrospinal fluid is predominantly through lymphatic vessels and is reduced in aged mice. Nat Commun. 2017;8(1):1434.
28. Aspelund A, Antila S, Proulx ST, Karlsen TV, Karaman S, Detmar M, et al. A dural lymphatic vascular system that drains brain interstitial fluid and macromolecules. J Exp Med. 2015;212(7):991–9.
29. Nagra G, Koh L, Zakharov A, Armstrong D, Johnston M. Quantification of cerebrospinal fluid transport across the cribriform plate into lymphatics in rats. Am J Physiol Regul Integr Comp Physiol. 2006;291(5):R1383-9.
30. Mathieu E, Gupta N, Macdonald RL, Ai J, Yücel YH. In vivo imaging of lymphatic drainage of cerebrospinal fluid in mouse. Fluids barriers of the CNS. 2013;10(1):35-.

Figures

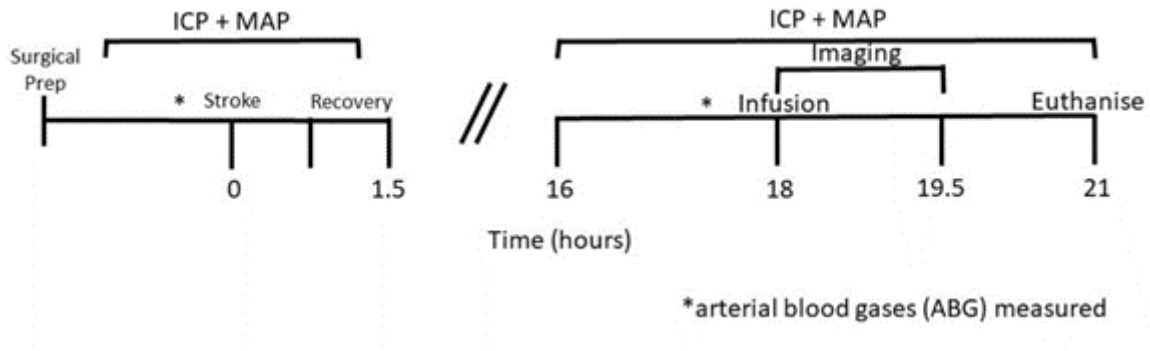

Figure 1

Experimental timeline. Lateral ventricle screw insertion and physiological variable recordings were carried out prior to stroke. Evans blue was infused 18-hours post-stroke and imaging was carried out 0- to 90-mins post-infusion. Day 1 physiological variables were recorded from 16- to 21-hours post-stroke. ICP = intracranial pressure, MAP = mean arterial pressure, * time point at which arterial blood gases (ABG) measured.

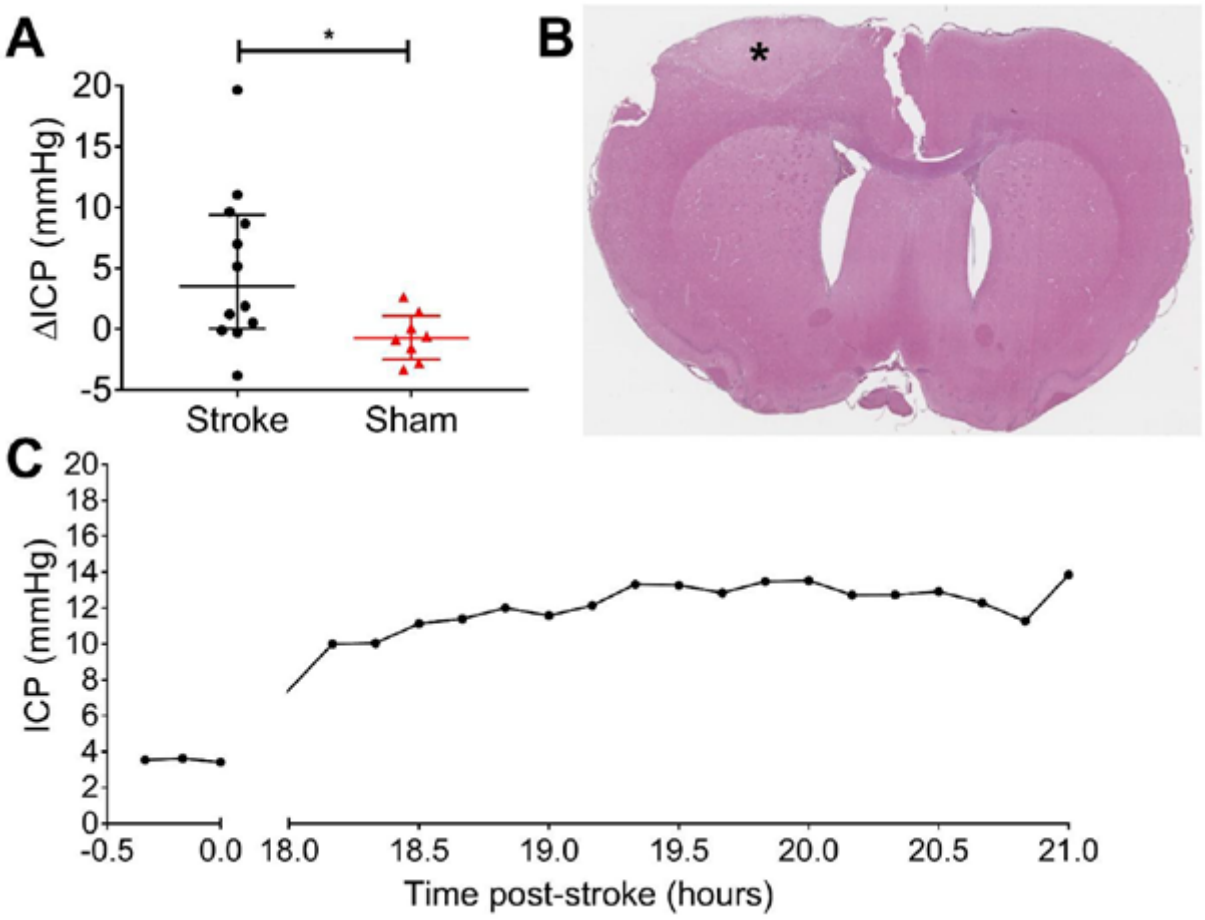

Figure 2

A) Change in ICP from day 0 to day 1 (18-hours post-stroke) in stroke (n = 12; circles) rats and in sham (n = 8; triangles) rats. *p≤0.05. B) Representative image of cortical ischaemia on right hemisphere after H&E

staining (Bregma +0.2). * indicates infarct. C) Representation of ICP at baseline and rising at 18- to 21-hours post-stroke in one animal. Representative images are from animal EB46. Change in ICP is presented as median and interquartile range.

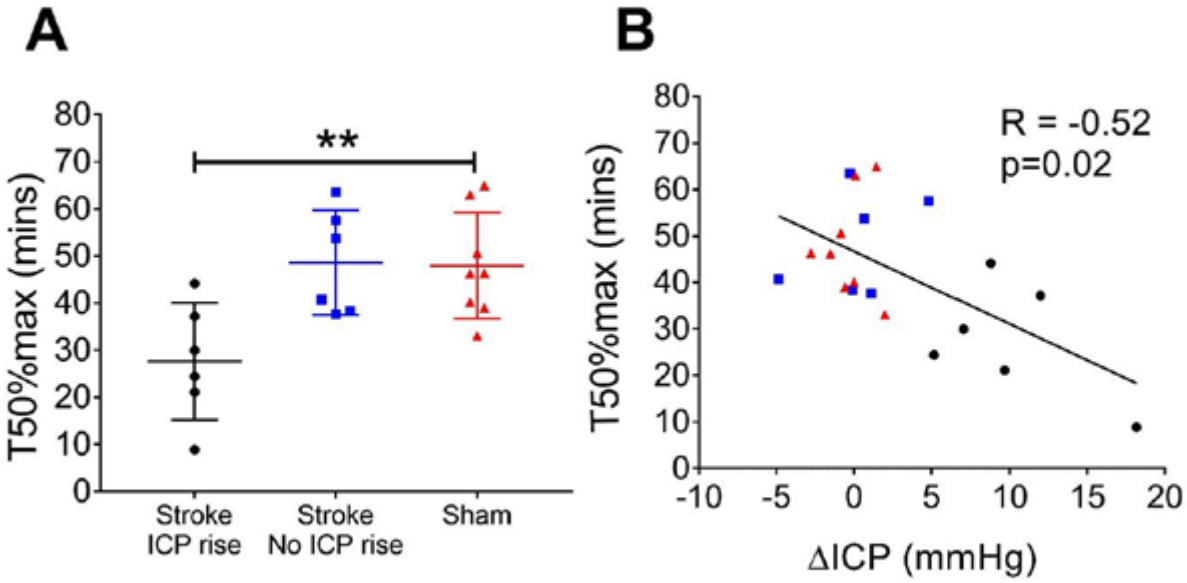

Figure 3

Time to reach 50% maximum contrast was determined for each animal. A) Time taken to reach 50% maximum contrast is shown for each group. **p≤0.01. B) Relationship between ΔICP and time taken to reach 50% maximum contrast. A Spearman's correlation was used to determine the relationship

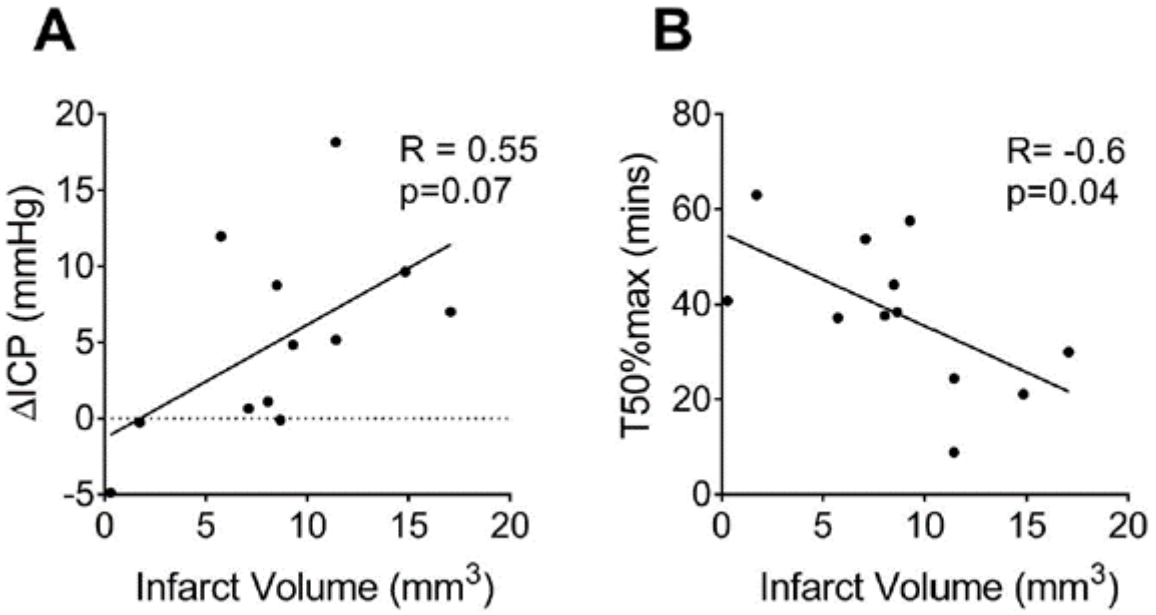

Figure 4

A) Relationship between infarct volume (mm3) and ΔICP between baseline and 18-hours post-stroke. A Spearmans correlation was used to determine the relationship. B) Relationship between infarct volume and time to 50% max contrast (mins). Individual animal data was plotted for animals subjected to photothrombotic stroke.

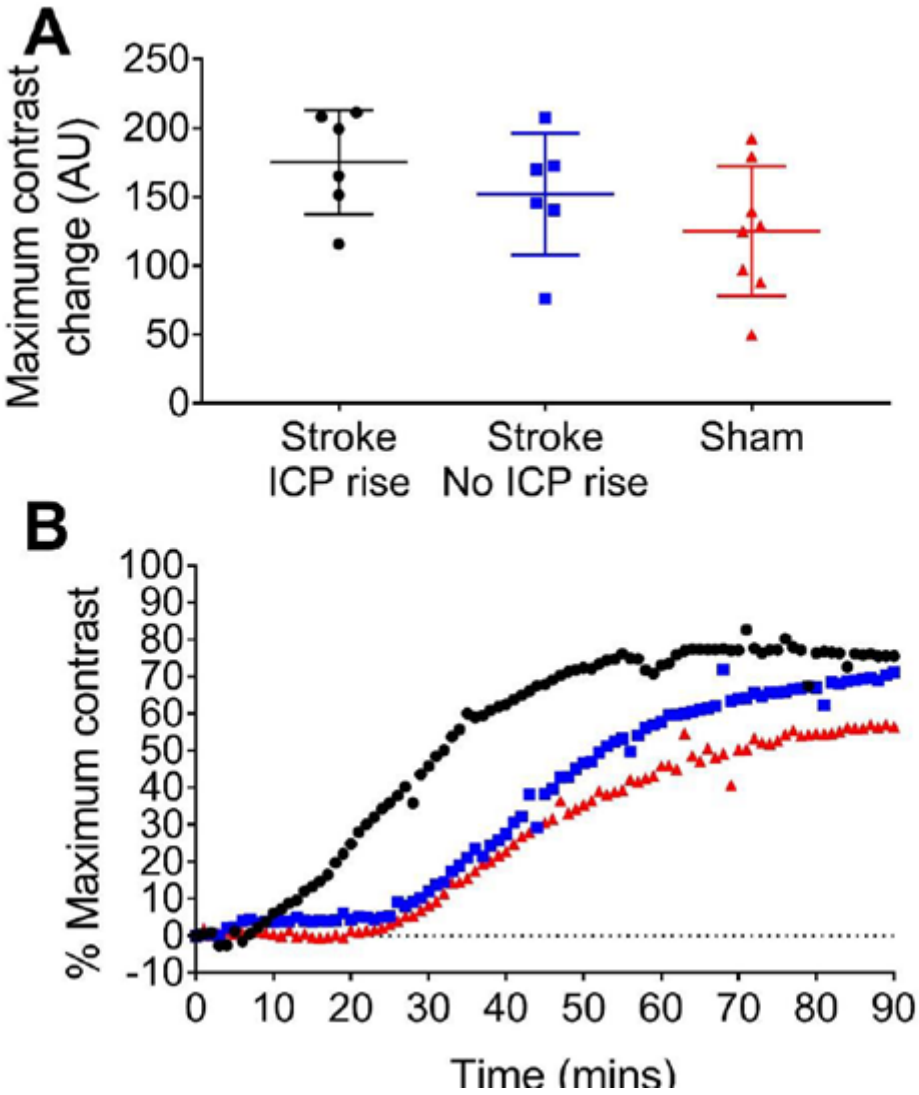

Figure 5

A) Oedema volume (mm3) plotted against ΔICP (mmHg) from baseline to 18-hours post-stroke. A Spearman's correlation was used to determine the relationship. B) Oedema volume plotted against time to 50% max contrast (mins). Individual animal data are shown for stroke animals (n = 12).

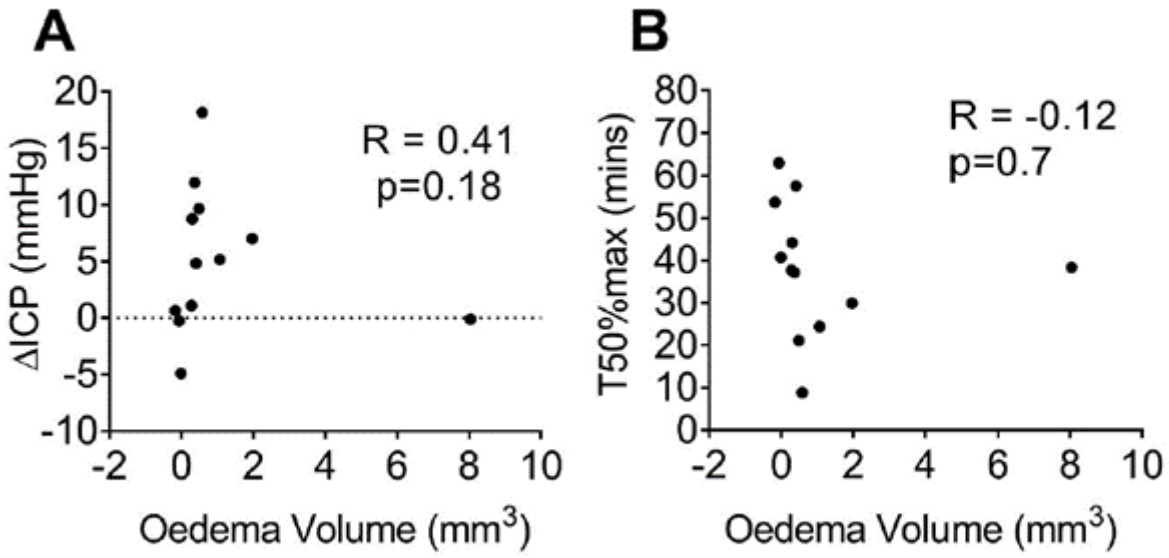

Figure 6

Maximum change in contrast from 0- to 90-mins post-infusion for stroke rats with ICP rise (≥ 5 mmHg; circles), stroke rats without ICP rise (squares), and sham rats (triangles). A) Maximum change in contrast for stroke rats with ICP rise (n = 6), stroke rats without ICP rise (n = 6), and sham (n = 8). B) Visual representation of contrast development between groups. Every data point at each 1-minute interval was averaged and plotted as a percentage of the maximum contrast value observed across all animals.